Nucleosomal Arrays Can Be Salt-Reconstituted on a Single-Copy MMTV Promoter DNA Template: Their Properties Differ in Several Ways from Those of Comparable 5S Concatameric Arrays†

R. Bash,‡,§ H. Wang,‡ J. Yodh,|| G. Hager,⊥ S. M. Lindsay,‡ and D. Lohr*,§

Department of Physics and Astronomy and Department of Chemistry and Biochemistry, Arizona State University, Tempe, Arizona 85287, Division of Basic Sciences, Arizona College of Osteopathic Medicine, Midwestern University, Glendale, Arizona 85308, and Laboratory of Receptor Biology and Gene Expression, Building 41, Room B602, National Cancer Institute, National Institutes of Health, Bethesda, Maryland 20892

Received September 21, 2002; Revised Manuscript Received March 3, 2003

ABSTRACT: Subsaturated nucleosomal arrays were reconstituted on a single-copy MMTV promoter DNA fragment by salt dialysis procedures and studied by atomic force microscopy. Up to an occupation level of approximately eight nucleosomes on this 1900 bp template, salt reconstitution produces nucleosomal arrays which look very similar to comparably loaded 5S rDNA nucleosomal arrays; i.e., nucleosomes are dispersed on the DNA template. Thus, at these occupation levels, the single-copy MMTV template forms arrays suitable for biophysical analyses. A quantitative comparison of the population features of subsaturated MMTV and 5S arrays detects differences between the two: a requirement for higher histone levels to achieve a given level of nucleosome occupation on MMTV templates, indicating that nucleosome loading is thermodynamically less favorable on this template; a preference for pairwise nucleosome occupation of the MMTV (but not the 5S) template at midrange occupation levels; and an enhanced salt stability for nucleosomes on MMTV versus 5S arrays, particularly in the midrange of array occupation. When average occupation levels exceed approximately eight nucleosomes per template, MMTV arrays show a significant level of mainly intramolecular compaction; 5S arrays do not. Taken together, these results show clearly that the nature of the underlying DNA template can affect the physical properties of nucleosomal arrays. DNA sequence-directed differences in the physical properties of chromatin may have important consequences for functional processes such as gene regulation.

Chromosome structure plays a critical role in the processes of replication, repair, and transcription in eukaryotes. The past 25 years have seen tremendous progress in our understanding of the basic elements of this structure, nucleosomes and nucleosomal arrays (*1*−*8*). Nucleosomal arrays are the foundation of *in vivo* chromosome organization. Therefore, studies of their intrinsic properties provide insights into this fundamental level of organization, as well as information about nucleosome structure that cannot be obtained from studies of individual nucleosomes (*1*, *8*, *9*).

In vitro reconstitution of nucleosomal arrays that are suitable for a wide range of studies has proven to be difficult. Salt reconstitution techniques, which can provide core mononucleosomes that are indistinguishable from those isolated from nuclear chromatin (*10*), typically produce arrays that are not considered suitable for study (*11*), due to inappropriate spacing of the nucleosomes (*12* and references therein). Incubation of such arrays with linker histone and polyglutamic acid (*13*) or the use of extracts or complexes isolated from cells to mediate *in vitro* assembly (*14*−*16*) can produce arrays in which the nucleosomes are appropriately spaced. However, the former method precludes studies of linker histone-free arrays, while the material produced by the latter approaches is not clean enough for many biophysical analyses. The development of concatameric DNA constructs (*17*) based on a nucleosome positioning sequence derived from the sea urchin 5S rDNA[1] gene (*18*−*20*) provides a template that can be salt-reconstituted into arrays of spaced nucleosomes. These arrays have proven to be suitable for most biophysical or biochemical studies, at saturated or subsaturated occupation levels (*1*, *8*, *21*, *22*). Nucleosome assembly on this template follows the order that is observed *in vivo*, first the H3−H4 tetramer, followed by one H2A−H2B dimer and then the other (*22*). For this and other reasons, these arrays are considered to be valid models for the polynucleosomal arrays that are the basic organizational unit of eukaryotic chromosome structure.

Our labs have been using atomic force microscopy (AFM) to study the population and locational aspects of nucleosome occupation at subsaturating levels on two of the 5S arrays,

† Financial Support to R.B., H.W., S.M.L., and D.L. (Grant CA-85990) is gratefully acknowledged.

* To whom correspondence should be addressed. Fax: (480) 965-2747. Phone: (480) 965-5020. E-mail: dlohr@asu.edu.

‡ Department of Physics and Astronomy, Arizona State University.

§ Department of Chemistry and Biochemistry, Arizona State University.

|| Midwestern University.

⊥ National Institutes of Health.

[1] Abbreviations: AFM, atomic force microscopy; rDNA, ribosomal DNA.

10.1021/bi026887o CCC: $25.00
Published on Web 04/03/2003

the 208-12 (*23*, *24*) and the 172-12 (*25*; R. Bash et al., manuscript in preparation). AFM is a powerful imaging technique that can be used to study many types of nucleic acid and nucleoprotein complexes (*26*, *27*), including chromatin isolated from cells (*28*−*31*) or reconstituted *in vitro* (*23*−*25*, *32*−*34*). AFM offers major advantages for chromatin studies. Single-molecule resolution allows a precise characterization of specific features, like the number of nucleosomes on individual arrays, and by analyzing many molecules, the statistical distribution of the feature of interest within a population. Subsaturated arrays are particularly useful in these types of studies because of the occupancy choices such templates offer and because there is less ambiguity in their quantitative AFM analysis than for saturated arrays. They also have some interest as models for newly replicated DNA and for the chromatin structure on gene promoters (*35*) and replication origins (*36*, *37*), which are not always fully nucleosome-saturated. Another strength of AFM is the ability to image in solution. This makes it possible to monitor the response of individual molecules under changing environmental conditions, for example, as the salt concentration is increased (*38*), and should be particularly important for structurally complex molecules such as chromatin, which undergo interactions with numerous factors (transcriptional regulators, remodeling factors, and modification enzymes).

While the 5S rDNA templates have proven to be a useful model for *in vitro* studies of nucleosomal arrays, their repetitive nature is not a feature shared by most functionally important eukaryotic DNA fragments, for example, gene promoter sequences. It would therefore be of considerable interest to be able to generate arrays that are as suitable for biophysical or biochemical analyses as the 5S arrays using such single-copy DNA templates. This paper provides AFM results showing that, at least at subsaturating occupation levels, analyzable arrays can be salt-reconstituted on an ~1.9 kb single-copy DNA fragment that contains the MMTV promoter. The MMTV promoter has long provided one of the premier models for nucleosome structure and nucleosome remodeling in response to gene activation, both *in vivo* (*39*, *40*) and *in vitro* (*41*, *42*). Quantitative AFM analysis of the population features of these subsaturated MMTV arrays shows that they differ in several significant ways from comparably loaded 5S rDNA arrays, demonstrating that the nature of the DNA template can affect fundamental chromatin properties. Array properties can also depend on the nucleosome occupation level.

MATERIALS AND METHODS

Chromatin Reconstitution. 172-12 and 208-12 DNA were isolated from plasmids p5S172-12 and pPol I, which were generous gifts from J. Hansen. The MMTV DNA used was an *Nco*I−*Sph*I fragment isolated from plasmid pGEM-3ZFM-LTRCAT, a generous gift from T. Fletcher. This 1863 bp fragment contains 400 bp of CAT DNA and 1500 bp of viral sequence, including the entire MMTV promoter region. Unacetylated HeLa histone octamers were prepared as previously described (*23*). The MMTV templates were reconstituted in sets of three or four samples. One sample (the "master"), containing the highest histone:DNA ratio of the set, was mixed in 2 M NaCl/TE, and then aliquots were removed and mixed with solutions (2 M NaCl/TE) containing the appropriate amounts of DNA needed to obtain the (lower) histone:DNA ratios chosen for each sample. Final concentrations of DNA were maintained at a constant level (0.1 μg/μL) within and among the various sets of reconstitutes. This method of sample preparation seems to yield more reproducible loading results than mixing each sample separately. Reconstitution utilized a stepwise dialysis from 2 M NaCl to a low ionic strength as follows: 1.6 M NaCl (3 h), 1.3 M NaCl (3 h), 1.0 M NaCl (for at least 6 h). 0.8 M NaCl (3 h), 0.6 M NaCl (for at least 6 h), and 1 mM EDTA (overnight). Samples were glutaraldehyde-fixed as described previously (*25*). The chromatin samples were dialyzed against fresh 0.1% glutaraldehyde in 1 mM EDTA (pH 8.0) for 6 h. Excess glutaraldehyde was removed by a final dialysis for 24 h against 1 L of 1 mM EDTA (pH 8.0). Reconstituted samples are routinely checked by electrophoresis on native 3.5% polyacrylamide gels. Array mobility on these gels depends on the nuclesosome occupation level, and this assay provides a surprisingly accurate, qualitative check on reconstitution (R. Bash et al., unpublished results).

Deposition and Imaging of Nucleosomes. Samples of reconstituted, fixed arrays were deposited on APTES (aminopropyl triethoxysilane) or GD-APTES surfaces. The APTES surface is made as described previously (*38*). To make GD-APTES, 200 μL of a 1 mM glutaraldehyde (grade I, Sigma-Aldrich, St. Louis, MO) solution in water is pipetted onto APTES-mica immediately after its removal from storage (desiccator under argon) and incubated on the surface for 10 min. The surface is rinsed with water (Nanopure ultrapure water system), and then 60 μL of a chromatin solution (diluted to 0.4 ng of DNA/μL in water) is pipetted onto the treated surface and allowed to incubate for 30 min. The surface is then rinsed again with water. For tapping mode imaging, the sample is air-dried and imaged as previously described (*25*). The images are taken in air with a Multi-Mode SPM instrument equipped with an E-scanner (Digital Instruments, Inc., Santa Barbara, CA) operating in the tapping mode. NanoProbe TESPprobes (Digital Instruments, Inc.), conical sharp silicon tips (NCH, Nanosensor), and V-shaped silicon cantilevers from K-Tek International, Inc., are used for imaging. The typical tapping frequency was 300−340 kHz for TESP tips and 340−380 kHz for the K-Tek probes; the scanning rate was 2−3 Hz. For solution imaging (e.g., the salt titrations), the prepared sample is mounted into an SPM liquid flow cell (Molecular Imaging, Phoenix, AZ), and NaCl solutions with increasing concentrations are injected into the flow cell *in situ*. Solution imaging was carried out with a Macmode PicoSPM (Molecular Imaging) equipped with triangular Si_3N_4 cantilevers (Molecular Imaging) with a spring constant of 0.1 N/m. Measurements were performed at a driving frequency of ~8 kHz and an oscillation amplitude of 5 nm with an 8% amplitude reduction. The scanning rate was 1.78 Hz.

Counting the Number of Nucleosomes. For each reconstituted sample, nucleosome numbers on at least 150 array molecules were determined. Molecules to be counted had to have distinguishable nucleosomes and discernible template termini. Every acceptable molecule in a field was counted. Nucleosome population distributions were obtained by plotting the fraction of molecules with a given number of nucleosomes (n) versus n. Distributions (n_{av}) ranged from <2 to $\cong 8$ (or more for the 5S array). n_{av} is the average

number of nucleosomes present on the templates in a sample distribution, calculated according to the equation

$$n_{av} = \frac{\sum_n nN_n}{\sum_N N_n}$$

where N_n is the number of molecules with n nucleosomes and the denominator is the total number of molecules counted.

RESULTS

AFM Images of Reconstituted MMTV Nucleosomal Arrays. The primary focus of these studies is an ~1900 bp, single-copy DNA fragment that contains the MMTV promoter region. Nucleosomal arrays with various subsaturating levels of occupation were reconstituted on this template, by varying the ratio of HeLa histone octamer to DNA, using a stepwise salt dialysis protocol like that used previously to produce subsaturated 208-12 and 172-12 chromatin samples for AFM studies (*23*−*25*). 5S arrays were also made and analyzed in parallel along with every set of MMTV reconstitutions in this work, as controls and reference points for all aspects of the analysis.

Representative AFM images of reconstituted MMTV arrays are shown in Figure 1 (panels A, C, and E). These three samples are from a single set of reconstitutions, made by appropriate dilutions of one master sample (Materials and Methods). As the images demonstrate, the nucleosome occupation level on the arrays clearly reflects the increasing histone inputs within the set. Array molecules are typically well-spread and individual nucleosomes clearly visualized. Nucleosomes generally distribute themselves along the template and show no tendency for extensive clustering. These MMTV arrays are as clearly visualized, and thus as easily analyzed, as either type of 5S array (Figure 1). Indeed, the two are qualitatively indistinguishable in appearance. Therefore, at these occupation levels, the MMTV template can be salt-reconstituted into nucleosomal arrays that are as suitable for *in vitro* studies as the 5S template. In this work, the population features of these salt-reconstituted MMTV arrays are characterized, by analysis of the types of images shown in Figure 1, to obtain (i) the population distribution, the number of molecules with n nucleosomes as a function of n, and (ii) n_{av}, the average number of nucleosomes per template (Materials and Methods) for each sample. Locational features, i.e., where the nucleosomes lie on the template, will be discussed elsewhere.

Response of Template Loading to Input Histone. The ability to count precise numbers of nucleosomes on the individual arrays in a sample allows a quantitative determination of the response of template loading to input histone. Such data contain fundamental thermodynamic information about histone−DNA association on these multi-binding site templates. Figure 2 shows the results of such a determination, plotted as n_{av} versus input histone (expressed as the molar ratio of octamers to DNA template molecules), for both MMTV and 5S (172-12 and 208-12) samples. The 5S data include the samples made in this study as well as samples previously analyzed (*23*, *25*).

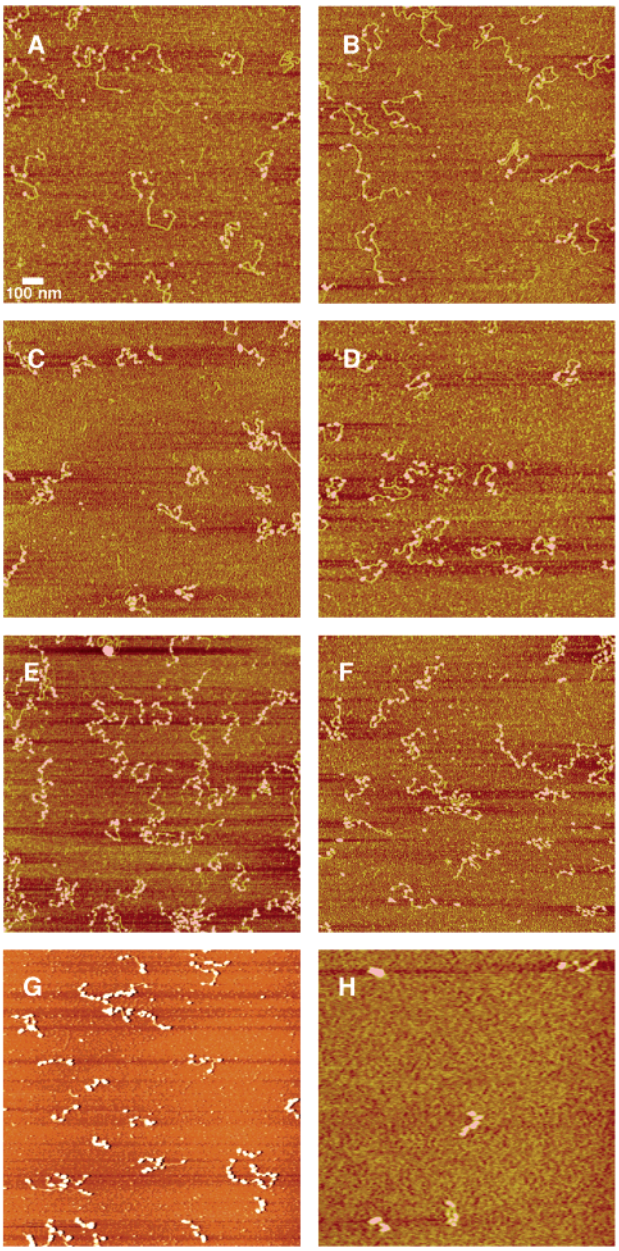

FIGURE 1: AFM images of MMTV and 5S nucleosomal arrays. Tapping mode (in air) images of subsaturated MMTV array samples with n_{av} values of 4.7 (A), 7.4 (C), and 8.8 (E) or 5S array samples with n_{av} values of 5.2 (B), 7.0 (D), and 9.3 (F) are shown. Panel B is a 208-12 sample, while panels D and F are 172-12 samples. Panel G shows a MacMode (solution) image of the same sample whose tapping mode image is shown in panel E, an MMTV sample with an n_{av} of 8.8. Panel H shows an example of a clumped MMTV sample (octamer:DNA ratio of 16:1 in the reconstitution). Samples shown in panels A−F and H were deposited on APTES-mica; panel G shows a sample deposited on GD-APTES.

The data show a good deal of scatter, which is probably due to the many variables associated with reconstitution. Nevertheless, it is apparent that a higher histone input is required to achieve a given n_{av} on the MMTV than on the 5S template, at all input levels. Thus, it is thermodynamically more difficult to load nucleosomes on the MMTV template in salt reconstitutions. Salt reconstitutions are thought to reflect equilibrium conditions (*43*, *44*), so this difference should reflect equilibrium properties of these DNA templates. Loading curves for the two 5S templates, 172-12 and 208-12, are similar. For all three DNA templates (MMTV, 172-

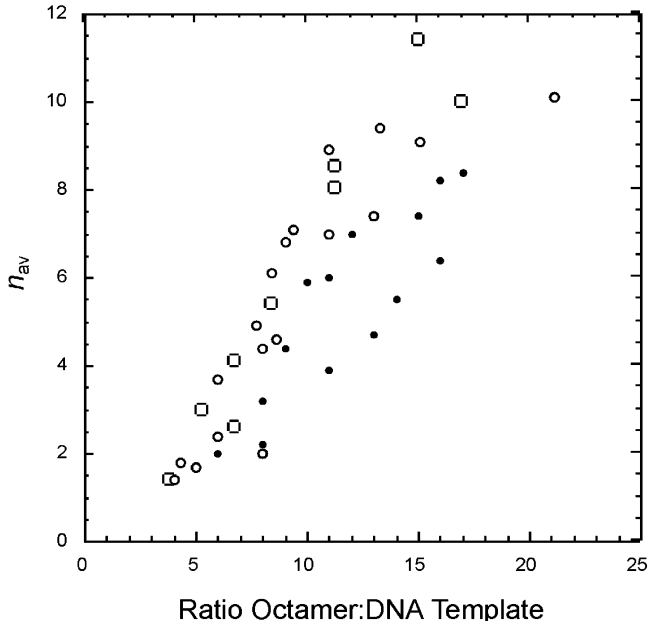

FIGURE 2: Response of template loading to input histone. The n_{av} of MMTV and 5S reconstituted samples is plotted vs the input histone octamer level, expressed as a molar ratio of octamer to DNA template, for MMTV samples (●), for 172-12 samples (○), and for 208-12 samples (□). The n_{av} values were determined from the types of tapping mode images shown in Figure 1 and are calculated as described in Materials and Methods.

12, and 208-12), the n_{av} value increases continuously with increasing input histone, as it should.

Both mixed sequence (*45*) and 5S (*46*) mononucleosomal length DNA templates load nucleosomes at efficiencies of ~80% in salt dialysis reconstitutions. On the basis of this efficiency, the 5S templates (12 nucleosome binding frames) should fully saturate by input histone levels of 15, as should the MMTV template, if 12 nucleosomes (the highest number we routinely observe) are also saturating on this template. The 208-12 template indeed approaches saturation at these input histone levels, but MMTV arrays are clearly much less than fully saturated, again indicating that it is inherently more difficult to load nucleosomes on this template. The MMTV template is somewhat shorter (~1900 bp) than the 208-12 (~2500 bp) or the 172-12 (~2100 bp), but these length differences are not likely to be responsible for the loading differences because the 208-12 and 172-12 templates differ significantly in length and yet are very similar in loading.

The precise response at very low loading levels ($n_{av} < 1$) is uncertain (*25*). Linear extrapolation of the curves would result in a non-zero *x*-axis intercept, suggesting that nucleosomes appear on the templates only after some minimum histone input has been exceeded, an effect most likely to arise from trivial features such as a need to saturate nonspecific binding sites on dialysis tubing. These low-input reconstitutions contain <1 μg of histone and thus might be expected to exhibit such behavior. Alternatively, the curves could approach zero asymptotically, reflective of a sigmoidal response and consistent with studies that detect cooperativity in nucleosome occupation (*25*).

There are several possible sources of error associated with these measurements. Counting error, assessed by multiple counters analyzing the same samples, is fairly constant across the range of array occupations, averaging ≤ 0.5 n_{av} unit. To estimate the uncertainties associated with the other experimental procedures, n_{av} values for experiments that used the same or very similar histone inputs were compared. These errors ranged from ± 0.5 to ± 2 n_{av} units (at higher occupation levels).

At an average occupation level of approximately eight nucleosomes per template (input histone:DNA ratio of ~16:1), MMTV samples begin to show significant numbers of highly compacted molecules (Figure 1H). Compaction occurs sporadically at these histone levels but quickly becomes dominating as input levels increase further. Thus, approximately eight nucleosomes per template seems to be a threshold occupational level on MMTV arrays beyond which compaction becomes a major feature. Compaction clearly depends on occupation level. Samples made in the same set as the sample shown in panel H, but reconstituted at lower histone levels, did not show any compacted molecules (data not shown), as is typical for MMTV arrays at lower occupation levels (cf. panels A and C of Figure 1). On the other hand, compaction is not a major feature of 5S arrays at any occupation level. Even highly loaded 208-12 ($n_{av} > 11$) or 172-12 ($n_{av} > 10$) samples contain at most only a few such molecules, and they never dominate the population as they do in MMTV samples. Compaction makes it impossible to count nucleosome numbers; thus, we have no MMTV loading data at input histone levels of >17 ($n_{av} > 8$).

This effect is mainly intramolecular in nature, formation of discrete blobs that are larger than nucleosomes or, much more commonly, compaction of large sections or even the whole molecule (Figure 1H). Only occasionally is there intermolecular aggregation. Since samples are fixed and maintained at low ionic strengths (after reconstitution), it is likely that compaction occurs during the latter stages of the reconstitution (<0.6 M NaCl) and persists at low ionic strengths. The intramolecular contacts that cause compaction presumably involve N-terminal histone tail-mediated internucleosomal interactions within arrays. The persistence of the effect at low ionic strengths might indicate that those interactions have some nonelectrostatic contribution, a suggestion made from other types of analyses (*8*).

Other features, such as association of extra histone octamers with nucleosomes (*47*, *48*) or surface effects, could potentially contribute to compaction. Extra octamer loading might explain the larger than nucleosomal-sized particles sometimes observed in these samples. The presence of the surface might facilitate compaction in several ways, for example, by binding arrays at multiple sites that lie close together on the surface. However, compaction is not merely an artifact of the surface or of extra octamer loading because it is limited to MMTV samples and to those MMTV samples that exceed a minimum occupation level. These features clearly indicate that the effect is DNA template-dependent. Interestingly, the threshold level for MMTV compaction is close to the occupation levels required for a perhaps analogous solution reaction, folding of 5S arrays (*49*).

Population Distributions. Distribution data for the samples whose images appear in Figure 1A−F are shown in Figure 3A−C. As judged by the relative frequencies of the peaks and other species in the distributions, by Gaussian fits to the data (Figure 3A′−C′) and the half-widths of those fits (Figure 3D), comparably loaded MMTV and 5S samples

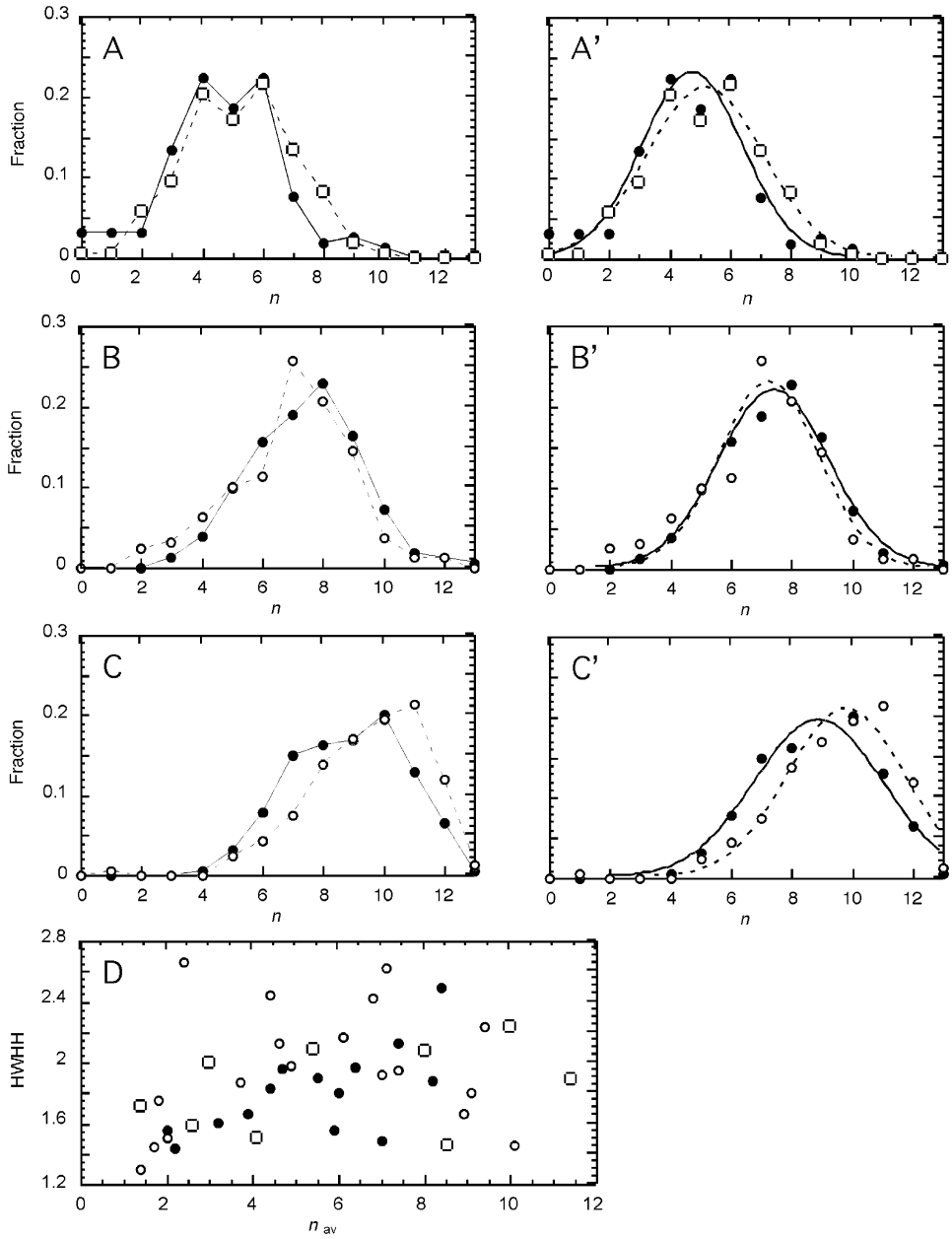

FIGURE 3: Population distributions. Panels A−C plot the fractions of molecules with a particular number (n) of nucleosomes vs n, for the reconstituted samples whose images are shown in panels A−F of Figure 1. The lines and dashes in panels A−C are only guides to the eye. Gaussian fits to the experimental results are shown in panels A′−C′. The filled circles (—) identify the MMTV samples, and the empty circles or squares (- - -) identify the 5S samples. Panel D shows a plot of the half-width at half-height (HWHH) of the distributions vs n_{av} for the complete set of MMTV (●) or 5S (○ or □) samples.

produce similar distributions across a range of occupation levels. Therefore, general population properties of individual MMTV and 5S samples do not differ significantly.

MMTV and 5S array populations do differ in two specific features.

(a) We noticed that all the peaks in the various MMTV sample distributions fell at an even number of nucleosomes (cf. panels A−C of Figure 3), which is not the case for the 172-12 (*25*) or 208-12 (*23*) samples, as Figure 3 also shows. To test for occupational correlations, the data were binned by n class, i.e., combining the numbers of molecules with three nucleosomes, with four nucleosomes, etc., from the entire data set, all the reconstituted MMTV samples whose n_{av} is greater than 3. This composite data set contains many more molecules than individual samples, thus increasing its statistical accuracy. Samples with very low n_{av} were excluded because they contain significant numbers of molecules with zero nucleosomes, which skews the data but does not alter the basic conclusion (not shown). As Figure 4 shows, MMTV arrays containing four and six nucleosomes are more prevalent than expected in the composite distribution, by >1 standard deviation (SD), whereas arrays with five and seven nucleosomes are less prevalent by >1 SD. Thus, the MMTV template shows a statistically significant tendency for occupation by even numbers of nucleosomes, i.e., a pairwise preference for occupation, in the midrange (from $n = 4$ to $n = 7$). Averaged over the entire distribution, the even bins contain an 18% (±7%) excess compared to the odd bins, translating into a free energy preference of 100 ± 40 cal/mol for loading of even numbers of nucleosomes on this

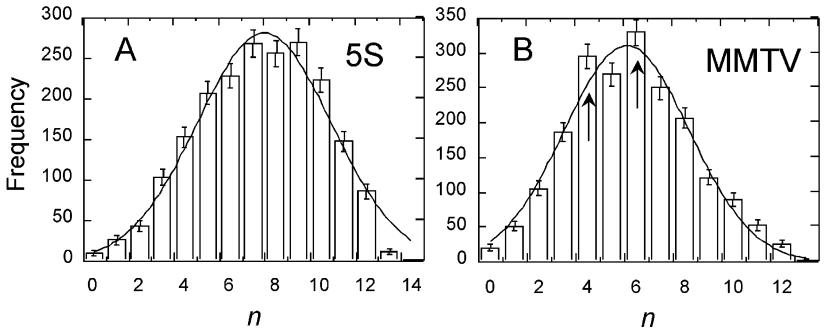

FIGURE 4: MMTV arrays demonstrate a tendency toward even numbered nucleosome occupation. The frequency of occurrence (numbers) of molecules with one, two, three, etc., nucleosomes is plotted vs the number of nucleosomes, *n*. These results represent compilations of data from the entire 172-12 data set (A) or the entire MMTV data set (B), i.e., all samples that were analyzed. The $n = 4$ and $n = 6$ arrays, i.e., arrays containing 4 and 6 nucleosomes, repectively, are identified with ascending arrows in the MMTV plot. The solid lines in both plots are fits to a skewed Gaussian. The error bars on each column represent ±1 SD.

template. The same analysis does not show such a tendency for 5S arrays (Figure 4); in fact, if anything, even-numbered occupation in the midrange appears to be slightly disfavored. The 172-12 data set contains more high n_{av} samples than the MMTV set, which accounts for the slight difference in distribution medians.

(b) The 172-12 distributions consistently display a peculiar nonrandom feature (*25*), a deficit in the number of molecules that contain one nucleosome more or less than the peak species in the distribution (whether the peak is even or odd). Although this feature is sometimes seen in individual distributions, it is not a consistent feature of MMTV samples, as judged from a composite made from all the MMTV data (not shown). Apparently, this anomaly is confined to 172-12 arrays.

Solution AFM Studies. To analyze single molecules in the solution state, samples are deposited on GD-APTES, a surface that is very well-suited for chromatin applications (*38*). This surface modification interacts with nucleosomes through the histones, but both the DNA and at least some histones maintain a significant degree of mobility even though they are surface-tethered.

Panel G of Figure 1 shows a solution image of the same MMTV sample whose air-dried image is shown in panel E. It is obvious that in the solution image nucleosomes and array molecules are as clearly visualized and thus as suitable for analysis as they are in the dried image. In samples whose n_{av} is greater than ~6, solution imaging does result in some nucleosome loss, reflected in a 5−25% lower n_{av} value compared to the same samples imaged in air. Loss occurs primarily from the more populated ($n > 6$) molecules in the distribution. It is due to the solution conditions and not the surface because air-dried samples have the same n_{av} values whether they are deposited on APTES or GD-APTES. Both 5S and MMTV arrays show the same behavior; thus, it probably reflects a general feature, perhaps nucleosome sliding off the template ends. Indeed, even mononucleosomes spontaneously dissociate to a small degree under these low-ionic strength conditions (*10*). Nucleosome loss is another indication of the mobility these samples maintain under solution imaging conditions; as expected, it is more extensive in unfixed samples (*38*).

The image quality permits detailed analyses of the solution state properties of these arrays. For example, previous solution AFM studies (*38*) detected decreases in nucleosome size at low NaCl concentrations (<0.6 M), consistent with a loss of the H2A−H2B dimer, and complete DNA loss from individual nucleosomes and eventually from entire arrays at higher NaCl concentrations. Both reactions are known to occur in solution on mononucleosomes (*10*) and arrays (*49*), although typically at somewhat higher NaCl concentrations than in the AFM studies. This difference could be due to an enhanced local salt concentration, a low nucleosome concentration near the surface, or direct physical effects of the surface on nucleosome stability.

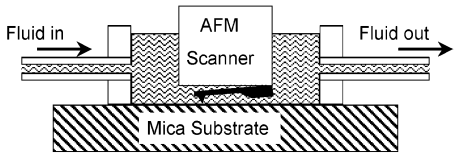

FIGURE 5: Diagram of the flow cell used for the salt stability experiments. The same set of tethered chromatin molecules is scanned by the AFM probe as the salt concentration in the liquid cell is changed by injecting new solutions.

Here, solution imaging is used to compare the salt stability of nucleosomes on MMTV and 5S arrays. To do this in a way that would allow the response of the same individual molecules to be followed as the NaCl concentration is increased, the analysis is carried out in a flow-through cell (Figure 5). This permits repeated scanning of the same area of the surface (and thus the same group of tethered molecules) as different salt solutions are passed through the cell. Figure 6A shows a typical "titration", the response of a number of individual nucleosomes (55 in this particular experiment, present on several subsaturated arrays) to increasing salt concentration. The sample n_{av} is 5.5. Nucleosomes in the sample begin to lose their DNA at ~0.4 M, but DNA release from all 55 nucleosomes is not complete until 1.0 M NaCl. The transition is rather sharp; ~75% of the molecules (43 of 55) lose their DNA between 0.7 and 0.85 M NaCl. For a comparable 5S sample, a 208-12 template with an n_{av} of 5.2, DNA dissociation starts at a lower NaCl concentration and is complete by 0.5 M, a salt concentration decidedly lower than the MMTV sample end point. Again, the transition is fairly sharp; ~65% of the molecules (26 of 40) lose their DNA between 0.3 and 0.4 M NaCl.

We have examined titration curves for a number of MMTV and 5S samples, at various n_{av} values. Although individual titrations vary in particular details, several features are consistently seen (Table 1). First, transition end point

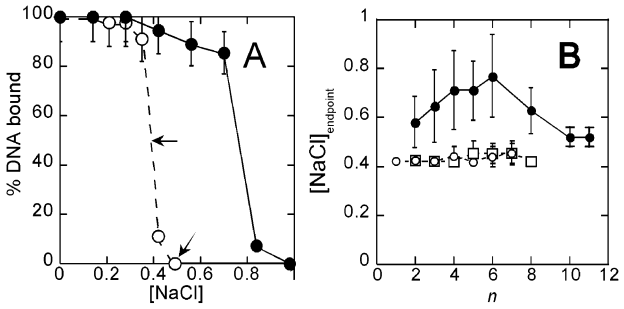

FIGURE 6: Salt stabilities of nucleosomes in MMTV and 5S nucleosomal arrays. (A) Typical salt titration curves, plots of the fraction of nucleosomes with DNA bound vs NaCl concentration, for various individual nucleosomes on several array molecules in an MMTV sample with an n_{av} of 5.5 (●) and a 208-12 5S rDNA sample with an n_{av} of 5.2 (○) are shown. The arrows point to the midpoint and the end point of the transition. (B) NaCl concentration required to reach the end point of the titration, i.e., the NaCl concentration at which all the single nucleosomes in an individual salt titration experiment have lost their DNA, is collated by *n* class, i.e., by the total number of nucleosomes (*n*) on the array, and plotted vs *n* [MMTV (●), 208-12 (□), and 172-12 (○)]. The data were compiled from salt titrations such as those shown in Figure 6A and include samples across the spectrum of n_{av} values that we have analyzed. The error bars are ±1 SD.

Table 1: Some Representative Salt Titration Results for MMTV and 5S Samples[a]

	n_{av}	midpoint [NaCl] (M)	end point [NaCl] (M)
MMTV	3.9	0.55	0.7
	5.5	0.8	1.0
		0.75	1.0
	9.1	0.5	0.7
5S			
208-12	5.2	0.35	0.5
172-12	7.0	0.35	0.5
172-12	9.5	0.35	0.4

[a] The NaCl concentrations at which 50% (midpoint [NaCl]) or 100% (end point [NaCl]) of the analyzed nucleosomes in a sample have released their DNA are shown for samples with varying n_{av} values. The n_{av} values that are given are the air-dried values. Only for n_{av} values of 9.1 (MMTV) and 9.5 (5S) are the solution values lower (~10% for the MMTV sample and ~25% for the 5S sample).

(or midpoint) values, i.e., the NaCl concentration required for 100% (or 50%) of the nucleosomes in the set of molecules to release their DNA, are consistently higher for the MMTV than for the 5S samples (Table 1). Second, these values vary with nucleosome occupation level for MMTV arrays; samples in the midrange ($n_{av} \sim 6$) show the highest values. In contrast, the data for 5S show no occupation level dependence. Both 5S arrays, 172-12 and 208-12, behave similarly. These data suggest that the salt stability of nucleosomes is greater in MMTV than in 5S arrays and is occupation level-dependent in the former.

For a more stringent test of these suggestions, the data from the entire MMTV sample set were combined and grouped by *n* class, i.e., the salt concentration required for DNA loss from nucleosomes residing in array molecules that contain a total of two nucleosomes, three nucleosomes, etc. Compiling the data in this way increases the numbers of molecules, thus enhancing the statistical accuracy, and provides an easy way to assess variance. Figure 6B shows these data, the NaCl concentration required for DNA loss from nucleosomes on arrays containing *n* nucleosomes, plotted versus *n*. For both types of 5S arrays, DNA loss is typically complete by <0.5 M and exhibits little dependence on the degree of array occupation. For MMTV arrays, NaCl concentrations of ≥0.7 M are required for complete loss from arrays with four to six nucleosomes but lower NaCl concentrations for release from arrays containing fewer than four or more than six nucleosomes. Thus, these data show the same trends seen in Table 1: the salt stability of nucleosomes is greater in MMTV than in 5S arrays, and it is occupation level-dependent, with arrays in the midrange ($n = 4-6$) showing the greatest stability. This analysis also shows that the variance is much higher in the MMTV than in the 5S data. Transition midpoints (sorted by *n* class) again show identical trends as the end points (not shown). Note that no molecules with seven or nine nucleosomes were found in the set of analyzed MMTV molecules.

The same extraneous features that could contribute to compaction (see above) might also affect the salt stability. For example, the presence and/or interaction of the surface with the arrays undoubtedly influences certain aspects of these salt titrations, for example, the absolute salt concentration at which changes occur. However, each type of array should be affected similarly. For example, surface attachment of the arrays occurs through the histones, and 5S and MMTV arrays were reconstituted with the same histones. Only the DNA template differs. Thus, as for compaction, the salt stability differences must reflect features unique to the template DNAs. The presence of extra octamers, if there are such, might be expected to make nucleosomes more salt stable. However, the extra octamers should be more prevalent at higher occupation (higher input histone) levels, and it is the less occupied (midrange) MMTV samples that show the highest level of salt stability. Also, only nucleosome-sized blobs were selected for the salt titration analysis, which should exclude nucleosomes with extra octamers. For all the above reasons, we feel that these comparative salt titration data provide valid indicators of relative salt stabilities of nucleosomes on the two types of arrays, at least when analyzed under these conditions (see below). The salt stability results seem to contradict the loading results (Figure 2). This point will be discussed below.

DISCUSSION

Subsaturated nucleosomal arrays were reconstituted by salt dialysis onto a single-copy 1900 bp DNA template containing the MMTV promoter and their population features characterized by AFM. The MMTV results were compared to results from a parallel analysis of subsaturated 172-12 and 208-12 5S rDNA arrays. AFM images, both in air and in solution, demonstrate that through a range of subsaturated occupation levels ($n_{av} \sim 2-8$), the MMTV DNA template can be salt-reconstituted into nucleosomal arrays that are as clearly visualized as and, indeed, qualitatively quite similar in appearance to, comparably loaded 5S arrays. Thus, up to an average occupation level of approximately eight nucleosomes on this single-copy DNA template, salt reconstitution produces arrays that are suitable for AFM or other biophysical or biochemical analyses.

Single-molecule precision and the ability of AFM to image in solution provide unique insights into the properties of MMTV and 5S arrays, including the detection of differences between them:

Loading. Higher histone levels are required to achieve a given occupation level on the MMTV than on the 5S template, indicating that it is thermodynamically more difficult to load the former. This may reflect a weaker average affinity of histones for MMTV DNA. MMTV (but not 5S) arrays also demonstrate a preference for even-numbered nucleosome occupation in the midrange (four and six nucleosomes per template). This could have at least two possible causes, internucleosomal interactions, perhaps of the closed pair type, or DNA torsional constraints between neighboring nucleosomes (*25*).

Compaction. As the occupation levels approach approximately eight nucleosomes per template (input histone:DNA ratio ~ 16:1), MMTV samples begin to show highly compacted array molecules; at increasing histone inputs, the effect quickly becomes dominating, and such samples consist largely of clumped, unanalyzable molecules. Thus, at levels that are less than saturating, compaction becomes a dominant effect for salt-reconstituted MMTV arrays. Such behavior is not observed with either type of 5S array, even at loadings that exceed those at which MMTV arrays are highly compacted. Although extraneous contributions such as excess octamer loading or surface-dependent effects might play a role in this behavior (see Results), the absence of major compaction in the 5S samples indicates that the MMTV behavior reflects a DNA template-dependent feature of these arrays.

The effect is mainly intramolecular and thus implies a high level of intraarray (internucleosomal) contact, probably mediated by the histone N-terminal tails. For example, acetylation of the tails mitigates the compaction behavior (R. Bash et al., manuscript in preparation). Histone tail-mediated effects, such as cooperativity in nucleosome occupation (*24*) and folding in solution (*1*), are observed in 5S nucleosomal arrays. Why do 5S arrays also not show strong compaction? AFM studies indicate that the cooperativity effects between nucleosomes in 208-12 arrays, even at their strongest, are only similar in magnitude to the positioning preferences exerted by the individual 5S rDNA units (*24*). Moreover, many of the favored nucleosome positions in these templates lie too far apart to allow the maximum cooperative interaction between neighboring occupied sites. Thus, in a sense, the positioning preferences are in competition with the cooperativity effects in these arrays. In 172-12 arrays, cooperativity should be enhanced because, on average, favored nucleosome positions lie closer, allowing the stronger levels of internucleosomal interaction. Although compaction is somewhat enhanced in 172-12 arrays, it never approaches the levels seen with MMTV. Apparently even in this template, positioning preferences imposed by the individual, strong histone binding 5S units still moderate the cooperativity of tail-mediated internucleosomal interactions enough to prevent extensive compaction. Thus, in both types of 5S arrays, nucleosomes on the individual rDNA units maintain some degree of independence, even though present in an array.

On the other hand, in templates with weaker inherent positioning preferences, such as the MMTV promoter (*50*−*52*), internucleosomal interactions can be a more dominant feature, allowing the nucleosomes in such arrays to behave more cooperatively via their internucleosomal contacts and thus leading to significant compaction as the template begins to fill up. Indeed, the extremely rapid onset of MMTV compaction suggests a cooperative effect. Pairwise occupational preferences at midranges of occupation (Figure 4) may also indicate enhanced levels of internucleosomal contact in MMTV arrays and could, in fact, reflect an early stage in the compaction process. The occupational threshold for compaction ($n_{av} > 8$) probably reflects a requirement that there are enough nucleosomes sufficiently close to each other, on average, to propagate internucleosomal contact. This threshold level is quite similar to the occupational threshold [estimated to be approximately nine nucleosomes per template (*49*)] for folding of 208-12 chromatin arrays in solution. The arguments above suggest (1) that internucleosomal interactions may exert even larger effects *in vivo*, in single-copy chromatin, than are seen in *in vitro* using models such as the concatameric 5S templates and (2) that chromatin regions containing positioning sequences, particularly if they are clustered, might behave quite differently from single-copy or nonpositioning regions with respect to cooperative effects such as folding. Suggestion 1 fits with arguments that a major role of chromatin-remodeling complexes is to loosen higher-order folding (*53*). With regard to suggestion 2, satellite DNAs could be an example of clustered positioning sequences whose function involves these types of differences in folding behavior.

Salt Stability. Perhaps the most novel results are provided by the studies that probe the salt stability of individual nucleosomes in arrays. These data show that stabilities are greater (DNA loss requires higher salt concentrations) for nucleosomes in MMTV than in 5S arrays. Also, stabilities in MMTV arrays depend on the array occupation level and show a large variance, implying a range of behaviors for these nucleosomes. In addition to a lower intrinsic stability, 5S stabilities do not vary with array occupation level and show a low variance, indicating a more limited behavioral range. These features are consistent with a more independent, autonomous nature for nucleosomes in 5S arrays, as suggested above. Both 5S templates show identical salt responses.

As discussed in the Results, the presence of the surface undoubtedly influences the salt stabilities of nucleosomes. However, it should affect each type of array similarly. Thus, although the environment for these salt studies is quite different from bulk solution conditions, the detection of significant stability differences between these otherwise similar array molecules indicates that there are real, template-specific physical differences between them. It is worthwhile noting that processes such as replication and transcription in cells probably occur mainly in large macromolecular "factories" located on the nuclear superstructure (*54*, *55*), in "crowded" cellular environments (*56*). Studies in dilute solution may be no more valid as models for those environments than reactions taking place on surfaces. Indeed, surface tethering might mimic the action of factors such as nucleosome remodeling complexes that interact with the histone component of nucleosomes in the course of carrying out their function.

Salt stability, as measured here, should reflect the inherent strength of the DNA−core histone interaction. The virtually identical stabilities for nucleosomes in the two 5S arrays, which contain the same basic (positioning) DNA sequence, are consistent with that suggestion. The greater salt stability

of nucleosomes in MMTV arrays would thus seem to indicate a stronger core histone−DNA interaction in that template. However, the loading results (Figure 2) suggest that the average DNA−histone affinity is lower in MMTV than in 5S arrays. Moreover, 5S DNA is known to bind histones more strongly than most DNA sequences (*43*, *57*), and although MMTV promoter DNA has not been directly evaluated in such binding studies, it would not be expected, on average, to bind histones more strongly than an array composed of strong 5S binding sites.

We cannot explain the apparently contradictory loading versus salt stability results. It may be that one of these behaviors is kinetically determined, but why these arrays would demonstrate kinetically based stability differences is also unclear. It may be that the two experiments reflect different aspects of stability; for example, a stronger histone binding DNA sequence exhibited less stability to nucleosome sliding in studies of MMTV mononucleosomes (*58*). Taken at face value, the data say that relative to 5S rDNA, MMTV DNA is less readily assembled into nucleosomes in solution (where both histones and DNA are free to move in three dimensions) but is less readily released from surface-tethered nucleosomes by salt. Release requires unspooling. This should depend on the torsional stiffness of the DNA, a highly sequence-dependent property that should be uncorrelated with histone binding ability. Surface tethering might also cause topological constraints involving extranucleosomal arrangements, which again could affect 5S and MMTV DNA sequences differently (*59*). Indeed, nucleosomes themselves can act as topological barriers in solution (*60*). Finally, arguments presented above suggest that the degree of internucleosomal interaction between 5S and MMTV arrays differs (due to the more independent nature for individual 5S nucleosomes), which could also contribute to nucleosome stability differences in the two types of arrays. Thus, DNA torsional or topological features and/or higher-order chromatin contributions may explain these differences in behavior.

Indeed, these contributions provide a rationale for explaining the occupation level dependence of the MMTV stabilities. Contributions to nucleosome stability from internucleosomal contacts should rise as the level of array occupation increases. In agreement with that expectation, nucleosomes in midrange occupied MMTV arrays ($n = 4-6$) are more stable than those in arrays with fewer nucleosomes (Figure 6). However, stability seems to decrease again in more highly occupied ($n > 6$) arrays. These more highly occupied arrays will have less free DNA than arrays in the midrange of occupation. Thus, midrange arrays should be better able to accommodate the torsional stress induced as salt begins to loosen the nucleosomal DNA, thereby prolonging its complete release. The weakened ability of the more highly occupied arrays to accommodate this stress could lower nucleosome stability, counteracting the expected contribution of enhanced internucleosomal interactions. The occupation level dependence of stability in MMTV arrays may also reflect the presence of DNA sites with differing histone affinities. Locational analyses (work in progress) should be able to detect such differences in affinity. The MMTV template clearly has some inherent heterogeneity, 400 bp of CAT DNA in addition to the ~1500 bp of MMTV sequence.

The differences in salt stability between MMTV and 5S arrays when analyzed under identical conditions, together with the loading (Figure 2) and population (Figure 4) differences, demonstrate quite clearly that the nature of the template DNA can affect the properties of nucleosomal arrays. The detection of differences between MMTV and 5S is strengthened by the near identity of the results for the two 5S templates. Clearly, the techniques that were used are inherently sufficiently precise to detect similar responses. The data also show that array properties can vary with occupation level; for example, arrays containing four to six nucleosomes have the most (salt) stable nucleosomes and also demonstrate a pairwise occupational preference. The novelty of the midrange and its potential importance in DNA replication were previously noted (*25*). Thus, although we cannot unambiguously interpret all the results presented here, the work does make two clear conclusions. (1) These very interesting and physiologically relevant DNA templates can be reconstituted *in vitro* into (subsaturated) arrays that are suitable for biophysical studies, and (2) the nature of the DNA template and its level of nucleosome occupation can greatly affect the properties of nucleosomal arrays. The kinds of quantitative, single-molecule studies described here will provide hitherto unobtainable insights into the basic properties of nucleosomal arrays. As these kinds of analyses continue, they should provide cogent explanations for the intrinsic properties of nucleosomal arrays.

REFERENCES

1. Fletcher, T., and Hansen, J. (1996) *Crit. Rev. Eukaryotic Gene Expression 6*, 149−188.
2. Widom, J. (1998) *Annu. Rev. Biophys. Biomol. Sruct. 27*, 285−327.
3. Workman, J., and Kingston, R. (1998) *Annu. Rev. Biochem. 67*, 545−579.
4. Wolffe, A., and Hayes, J. (1999) *Nucleic Acids Res. 27* (3), 711−720.
5. Kornberg, R., and Lorch, Y. (1999) *Cell 98*, 285−294.
6. Wolffe, A., and Guschin, D. (2000) *J. Struct. Biol. 129*, 102−122.
7. Hayes, J., and Hansen, J. (2001) *Curr. Opin. Genet. Dev. 11*, 124−129.
8. Hansen, J. (2002) *Annu. Rev. Biophys. Biomol. Struct. 31*, 361−392.
9. Hansen, J., Tse, C., and Wolffe, A. (1998) *Biochemistry 37*, 17637−17641.
10. Van Holde, K. (1988) *Chromatin*, Springer-Verlag, New York.
11. Rhodes, D., and Laskey, R. (1989) *Methods Enzymol. 170*, 575−585.
12. Stein, A., and Bina, M. (1984) *J. Mol. Biol. 178*, 341−363.
13. Jeong, S., Lauderdale, J., and Stein, A. (1991) *J. Mol. Biol. 222*, 1131−1147.
14. Wolffe, A. (1998) *Chromatin Structure and Function*, Academic Press, San Diego.
15. Adams, C., and Kamakaka, R. (1999) *Curr. Opin. Genet. Dev. 9*, 185−190.
16. Mello, J., and Almouzni, G. (2001) *Curr. Opin. Genet. Dev. 11*, 136−141.
17. Simpson, R., Thoma, F., and Brubaker, J. (1985) *Cell 42*, 799−808.
18. Simpson, R., and Stafford, D. (1983) *Proc. Natl. Acad. Sci. U.S.A. 80*, 51−55.
19. Dong, F., Hansen, J., and van Holde, K. (1990) *Proc. Natl. Acad. Sci. U.S.A. 87*, 5724−5728.
20. Meersseman, G., Pennings, S., and Bradbury, E. (1991) *J. Mol. Biol. 220*, 89−100.
21. Carruthers, L., Tse, C., Walker, K., III, and Hansen, J. (1999) *Methods Enzymol. 304*, 19−35.
22. Hansen, J., van Holde, K., and Lohr, D. (1991) *J. Biol. Chem. 266*, 4276−4282.

23. Yodh, J., Lyubchenko, Y., Shlyakhtenko, L., Woodbury, N., and Lohr, D. (1999) *Biochemistry 38*, 15756−15763.
24. Yodh, J., Woodbury, N., Shlyakhtenko, L., Lyubchenko, Y., and Lohr, D. (2002) *Biochemistry 41*, 3565−3574.
25. Bash, R., Yodh, J., Lyubchenko, Y., Woodbury, N., and Lohr, D. (2001) *J. Biol. Chem. 276*, 48362−48370.
26. Lyubchenko, Y., Jacobs, B., Lindsay, S., and Stasiak, A. (1995) *Scanning Microsc. 9*, 705−727.
27. Lindsay, S. M. (2000) The Scanning Probe Microscope in Biology, in *Scanning Probe Microscopy, Techniques and Applications* (Bonnel, D., Ed.) 2nd ed., John Wiley, New York.
28. Leuba, S., Yang, G., Robert, C., Samori, B., van Holde, K., Zlatanova, J., and Bustamante, C. (1994) *Proc. Natl. Acad. Sci. U.S.A. 91*, 11621−11625.
29. Martin, L., Vesenka, J., Henderson, E., and Dobbs, D. (1995) *Biochemistry 34*, 4610−4616.
30. Fritzsche, W., and Henderson, E. (1997) *Scanning 19*, 42−47.
31. Zlatanova, J., Leuba, S., and van Holde, K. (1998) *Biophys. J. 74*, 2554−2566.
32. Allen, M., Dong, X., O'Neill, T., Yau, P., Kowalczykowski, S., Gatewood, J., Balhorn, R., and Bradbury, E. (1993) *Biochemistry 32*, 8390−8396.
33. Sato, M., Ura, K., Hohmura, K., Tokumasu, F., Yoshimura, S., Hanaoka, F., and Takeyasu, K. (1999) *FEBS Lett. 452*, 267−271.
34. Schnitzler, G., Cheung, C., Hafner, J., Saurin, A., Kingston, R., and Lieber, C. (2001) *Mol. Cell. Biol. 21*, 8504−8511.
35. Lohr, D. (1997) *J. Biol. Chem. 272*, 26795−26798.
36. Sogo, J., Stahl, H., Koller, T., and Knippers, R. (1986) *J. Mol. Biol. 189*, 189−206.
37. Lohr, D., and Torchia, T. (1988) *Biochemistry 27*, 3961−3965.
38. Wang, H., Bash, R., Yodh, J., Hager, G., Lohr, D., and Lindsay, S. (2002) *Biophys. J.* (in press).
39. Hager, G., Smith, C., Svaren, J., and Hörz, W. (1995) In *Chromatin Structure and Gene Expression* pp 89−99, Oxford University Press, New York.
40. Hager, G. (2001) *Prog. Nucleic Acids Res. Mol. Biol. 66*, 279−305.
41. Fletcher, T., Ryu, B., Baumann, C., Warren, B. Fragaso, G., John, S., and Hager, G. (2000) *Mol. Cell. Biol. 20*, 6466−6475.
42. Fletcher, T., Xiao, N., Mautino, G., Baumann, C., Wolford, R., Warren, B., and Hager, G. (2002) *Mol. Cell. Biol. 22* (10), 3255−3263.
43. Shrader, T., and Crothers, D. (1989) *Proc. Natl. Acad. Sci. U.S.A. 86*, 7418−7422.
44. Lowary, P., and Widom, J. (1998) *J. Mol. Biol. 276*, 19−42.
45. Tatchell, K., and van Holde, K. (1977) *Biochemistry 16*, 5295−5303.
46. Luger, K., Rechsteiner, T., and Richmond, T. (1999) *Methods Enzymol. 304*, 3−19.
47. Stein, A. (1979) *J. Mol. Biol. 130*, 103−134.
48. Eisenberg, H., and Felsenfeld, G. (1981) *J. Mol. Biol. 150*, 537−555.
49. Hansen, J., and Lohr, D. (1993) *J. Biol. Chem. 268*, 5840−5848.
50. Richard-Foy, H., and Hager, G. L. (1987) *EMBO J. 6*, 2321−2328.
51. Fragoso, G., John, S., Roberts, M. S., and Hager, G. L. (1995) *Genes Dev. 9*, 1933−1947.
52. Roberts, M. S., Fragoso, G., and Hager, G. L. (1995) *Biochemistry 34*, 12470−12480.
53. Horn, P., and Peterson, C. (2002) *Science 297*, 1824−1827.
54. Hughes, T., Pombo, A., McManus, J., Hozák, P., Jackson, D., and Cook, P. (1995) *J. Cell Sci. 19*, 59−65.
55. Cook, P. (1999) *Science 284*, 1790−1795.
56. Ellis, R. (2001) *Curr. Opin. Struct. Biol. 11*, 114−119.
57. Gottesfeld, J., and Luger, K. (2001) *Biochemistry 40*, 10927−10933.
58. Flaus, A., and Richmond, T. (1998) *J. Mol. Biol. 275*, 427−441.
59. Yang, Y., Westcott, T., Pedersen, S., Tobias, I., and Olson, W. (1995) *Trends Biochem. Sci. 20*, 313−319.
60. Mondal, N., and Parvin, J. (2001) *Nature 413*, 435−438.

BI026887O